Real-Time Hydrogen Refuelling of the Fuel Cell Electric Vehicle Through the Coupled Transportation Network and Power System

Bei Li, *Member, IEEE*, Jiangchen Li, *Member, IEEE*, Zhixiong Li, *Senior Member, IEEE*, and Miguel Angel Sotelo, *Fellow, IEEE*

***Abstract*— At present, hydrogen fuel cell electric vehicle (HFCEV) is increasingly affordable to replace petrol vehicles and reduce carbon dioxide emissions. However, the refuelling of the HFCEV is still an essential problem. Specifically, there are not enough hydrogen refuelling stations at hand. In this paper, a hydrogen based microgrid is presented to produce hydrogen to refuel the HFCEV, and different strategies are proposed to guide the HFCEV's refuelling within the coupled transportation network and power system. First, the HFCEV traffic flow model based on a real-world transportation network is presented. Then, a real-time simulation platform links the Sumo and Matlab is presented. Third, a hydrogen based microgrid to refuel HFCEV is built. Forth, an IEEE 30-node utility grid exporting power model is presented. At last, the real-time hydrogen refuelling of HFCEV through the coupled transportation network and power system is proposed. Four coupled structures are considered, and different HFCEV refuelling strategies (fixed price, dynamic price, LSTM decision price) are compared. The simulation results demonstrate that with the dynamic price, the congestion of the transportation network is improved, the waiting time is reduced by 17.71%, and the time loss of the network is reduced by 13.29%. With reasonable guidance of the price, vehicles choose the selected station to refuel hydrogen and influence the temporal-spatial distribution of the traffic flow of the transportation network. In addition, by adjusting the power station exporting power and the refuelling station importing power, the voltage condition of the power system can be improved.**

***Index Terms*— Fuel cell electric vehicle, microgrid, hydrogen refuelling station, transportation network, real-time, power system.**

NOMENCLATURE

Acronyms

BPR	Bureau of Public Roads.
CO2	Carbon dioxide.
DFS	Depth first search.
HFCEV	Hydrogen fuel cell electric vehicle.
LOH	Level of hydrogen.
LSTM	Long short term memory.
OD	Origin-destination.
OPF	Optimal power flow.
PEM	Proton exchange membrane.
SOC	State of charge.
SUMO	Simulation of Urban MObility.

Manuscript received 21 July 2022; revised 26 May 2023 and 15 October 2023; accepted 20 May 2024. Date of publication 13 June 2024; date of current version 2 July 2024. This work was supported in part by Guangdong Basic and Applied Basic Research Foundation under Grant 2022A1515240034 and Grant 2019A1515110641, in part by the Fundamental Research Funds for Shenzhen University under Grant 000002110235, in part by Shenzhen High-Level Talents Project 000661, and in part by the National Science Centre of Poland under Project 2023/51/B/ST8/02275. The Associate Editor for this article was H. Khayyam. *(Corresponding author: Zhixiong Li.)*

Bei Li is with the College of Chemistry and Environmental Engineering, Shenzhen University, Shenzhen 518060, China (e-mail: bei.li@szu.edu.cn).

Jiangchen Li is with the College of Civil Aviation, Nanjing University of Aeronautics and Astronautics, Nanjing 211106, China (e-mail: jiangchen@nuaa.edu.cn).

Zhixiong Li is with the Faculty of Mechanical Engineering, Opole University of Technology, 45-758 Opole, Poland (e-mail: z.li@po.edu.pl).

Miguel Angel Sotelo is with the Department of Computer Engineering, University of Alcalá, 28801 Madrid, Spain (e-mail: miguel.sotelo@uah.es).

Digital Object Identifier 10.1109/TITS.2024.3409532

I. INTRODUCTION

AT PRESENT, transportation is responsible for a high percentage of greenhouse gas emissions. In 2022, transportation sector carbon dioxide (CO2) emissions reached a high of 7.98 Gt, which is about 21.7 % of the total emissions [1]. In Europe, the greenhouse gas emissions of the transportation sector are about a quarter of total emissions [2]. To reduce the CO2 emissions in the transport sector, the electric vehicle has been put forward on the agenda to replace the gasoline vehicle. Over the last decades, the number of battery electric vehicles has been increasing. However, battery electric vehicle has some disadvantages, including long charging time and limited driving range [2].

Nowadays, hydrogen fuel cell electric vehicle has been increasingly affordable, different types of HFCEV can be seen in [3]. Many countries, such as America, Japan, and European nations encourage the utilization of HFCEV on their roads [4]. Compared with the battery electric vehicle, HFCEV has a similar performance to conventional vehicles with regards to range and speed [4], and the quick refuelling of hydrogen, less than 5 min [5]. However, the promotion of HFCEV is highly dependent on the construction of hydrogen refuelling infrastructure, and not enough refuelling stations are prepared at present. Specifically, the construction cost for one hydrogen refuelling station is about ten times higher than that of a gas station [6].

The common structure of the off-site hydrogen refuelling infrastructure includes three parts, hydrogen production, hydrogen delivery, and hydrogen dispensing [7]. However, on-site renewable energy-powered hydrogen refuelling station is recently increasingly popular [8], in which, hydrogen is produced from renewable energy, and no greenhouse gas is emitted.

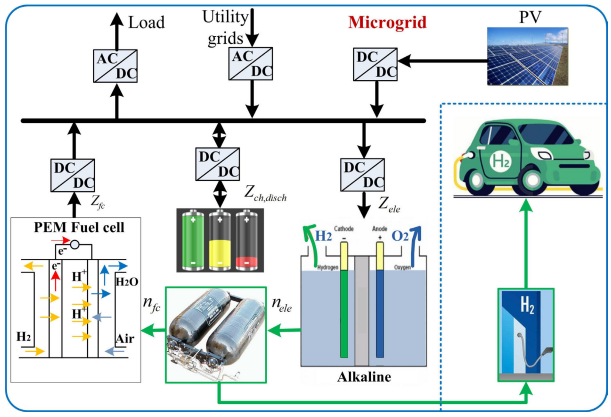

Fig. 1. Hydrogen based microgrid to produce hydrogen to refuel hydrogen fuel cell electric vehicles.

In this paper, a hydrogen based microgrid is built to produce hydrogen to refuel HFCEVs. The structure of the hydrogen based microgrid is presented in Fig. 1. In the microgrid, an electrolyzer is deployed to produce hydrogen through electrical power, and hydrogen is stored in tanks. Hydrogen can be used either to generate electricity through the fuel cell or to refuel HFCEVs through refuelling stations. Hydrogen based microgrid has been verified in a variety of situations [9].

Moreover, as the widely installed renewable energy resources around the world, using green electricity to produce hydrogen is the trend and can reduce costs, such as wind power [10], solar power [11], nuclear power driven electrolysis hydrogen production.

On the other hand, HFCEV travels on the transportation network and has a temporal-spatial characteristic. When a vehicle needs to refuel hydrogen, it needs to choose an appropriate refuelling station. First, it wants to travel to the nearest refuelling station to save time. Second, it wants to travel to the cheapest refuelling station to reduce costs.

Meanwhile, if lots of vehicles travel to the same refuelling station, which will then cause traffic congestion around the refuelling station, and also cause a peak hydrogen demand in the refuelling station. Thus, considering the real-time state of the transportation network and the power network to avoid traffic congestion and peak demand is an essential problem.

In this paper, a real-time HFCEV refuelling through the coupled transportation network and power system is proposed. The microgrid is deployed to link these two networks, and the structure of the transportation network, microgrid, and power system is presented in Fig. 2. The left network is an IEEE 30-node network, which can export electricity to a microgrid. The renewable energy based power station is deployed to supply renewable energy to the utility grid. The right network is a real-world transportation network, which is deployed to simulate the temporal-spatial hydrogen refuelling of the vehicles. The HFCEVs travel around and can refuel hydrogen in microgrids. Four microgrids are interconnected with the power network.

A. Hydrogen Refuelling of the Fuel Cell Electric Vehicle

In fact, refuelling of the HFCEV and the hydrogen refueller stations have been widely studied. For example, in [12], authors study a hydrogen refuelling station, which includes the electrolyzer stacks, storage, dispenser, cooling, and rectifier. The hydrogen demand of the HFCEV is modeled based on the arrival rate and the initial state of the on-board tank range. In [13], a renewable energy-based self-sustainable hydrogen refuelling station is presented, proton exchange membrane (PEM) electrolyzer is deployed to produce hydrogen. The hydrogen demand is obtained from measured data. In [14], wind turbine and utility grid are deployed to supply power to the PEM electrolyzer to build the hydrogen refuelling station, and time series hydrogen demand is derived from a simulated profile. In [15], a hydrogen filling station with a pressurized alkaline electrolyzer experiment system is presented. Wind turbines and solar panels are deployed to provide renewable energy. Different electrolyzer operation modes are compared.

A water electrolyzer can split water into hydrogen and oxygen using any electrical power source. For the commercial electrolyzer, the energy efficiency is about 55-75% [16]. And the renewable energy-driven water electrolyzer is increasing as the most common and widely used process. However, in the above papers, the authors do not consider the utility grid network operation and the transportation network vehicle traffic flow.

Interdisciplinary studies of the power network and transportation network coupling are desired, and lots of papers have been published. For example, in [17], the authors study the planning of urban electrified transportation networks, which determines the investment strategies for the transportation network and the power distribution network. Nesterov user equilibrium is used to describe traffic flow, and linearized branch power flow is adopted to derive the operation condition of the distribution network. In [18], the authors study the planning of electric vehicle charging stations by coupling the transportation network with the power distribution network. The links between the two networks are charging demands, which are assumed to be a linear function of traffic flow. In [19], the authors study the coordinated operation of transportation systems and power systems. The problem is formulated as a centralized optimization problem, the objective function is to minimize the sum of the total travel cost of the transportation network and the energy service cost of the distribution network. In [20], authors study the robust operation of the coupled power distribution networks and urban transportation networks. The power demand load perturbation caused by the traffic demand uncertainty is considered.

However, at present, integrating renewable energy resources into the power network is an increasing trend. The above papers still focus on the traditional distribution network, and lack of investigations on the active distribution network.

In terms of the coupling of the active distribution network and transportation network, some work also has been done. In [21], the authors study the optimal planning of a coupled distribution network and transportation network, electric vehicle charging facilities are the links between these two networks. The charging demand is described as an increasing function subject to the traffic flow. Steady traffic flow assignment in the transportation network and conic relaxation-based branch flow in the distribution network are considered.

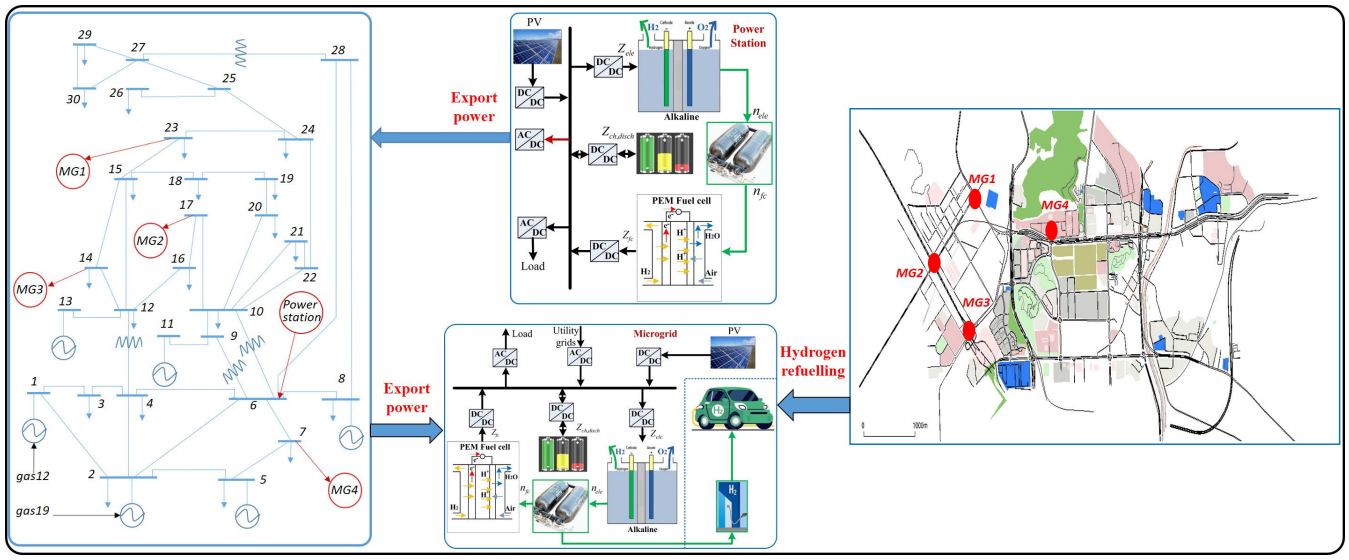

Fig. 2. The structure of the power station, power system network, microgrid, and transportation network.

Furthermore, in [22], the authors study the planning of the coupling of transportation, natural gas, and active distribution networks. Multi-energy stations are presented as coupling components. Traffic flow, power flow, and natural gas flow are considered. In [23], authors study the trading for multiple microgrids coupled with transportation networks. The fast charging stations are installed in microgrids and linked to the transportation network. The vehicles act to minimize their travel costs in response to the charging prices. The microgrid aims to minimize the operation cost via energy trading and electric vehicle charging.

However, the above papers all focus on electric vehicle charging, and the HFCEV refuelling still lacks investigations. Compared with the battery electric vehicle, the HFCEV has a short refuelling time, but typically, the hydrogen refuelling facilities need to consume auxiliary electricity power [24].

In addition, in the hydrogen refuelling stations, to better manage the refuelling vehicles, the customer refuelling behavior information needs to be considered. For example, in [25], the authors study the optimal operation of a hybrid hydrogen/electricity refuelling station powered by solar. The hydrogen refuelling demand is obtained from the recorded data. In [26], the authors study the operation of a grid-connected hydrogen refuelling station, which purchases power from the utility grid market. The hydrogen demands are obtained from a fuel station profile and adjusted based on the hydrogen demand for mobility in Belgium. In [27], the authors study the optimal scheduling of an IEEE 33-bus distribution microgrid with hydrogen refuelling stations taking into consideration of uncertainties. The hydrogen demands are obtained based on the forecast method. Moreover, in [28], authors study the refuelling behavior and derive demand profiles for car-sharing vehicles.

However, in the above papers, the temporal-spatial characteristic of the customer refuelling behavior is not considered. Especially, when considering the real-world transportation network, the refuelling behavior of HFCEVs is complex.

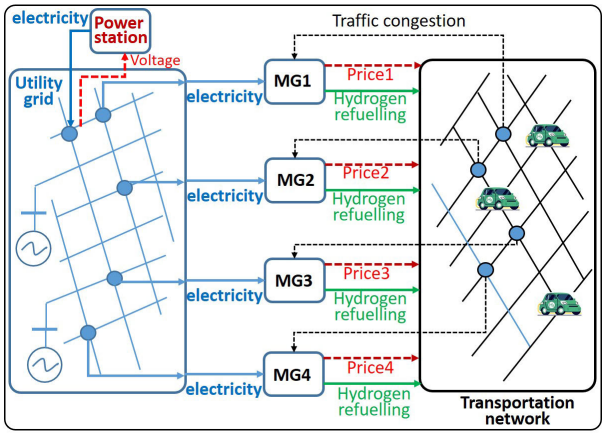

Fig. 3. The operation relations of HFCEV refuelling, microgrids, and utility grid.

In this paper, SUMO [29] traffic simulator is adopted to describe the HFCEV refuelling behavior through a real-world transportation network. HFCEVs choose the best refuelling station based on the travelling distance and the hydrogen selling price. Then, a hydrogen based microgrid is deployed to produce hydrogen to refuel vehicles, and in each microgrid, the hydrogen selling price can be adjusted based on the traffic network congestion. When the traffic around the microgrid is congested, then the hydrogen selling price is increasing, intending not to attract the consumers. At last, the microgrid can import electricity from the utility grid. Based on the utility grid voltage condition, the power station adjusts its output power to improve the utility grid operation condition. The operation relations of HFCEV refuelling, microgrids, and utility grid are presented in Fig. 3.

B. Contributions

Compared to the previous works, the contribution of this paper can be concluded as follows:

- First, the SUMO traffic simulator is adopted to model the HFCEV refuelling behavior through a real-world transportation network;
- Second, a hydrogen based microgrid is deployed to produce hydrogen to refuel vehicles and the hydrogen selling price is deployed to guide vehicles to stations to refuel hydrogen;
- Third, with the dynamic price, the congestion of the transportation network is further improved, and the waiting time and time loss of the network are further reduced;
- Forth, a long short-term memory (LSTM) network is deployed to train the relationship between states (voltage, traffic flow) and the price. And the hydrogen price is adjusted based on the smart LSTM network.
- Last, with reasonable guidance of the price, vehicles choose the cheapest station to refuel hydrogen and influence the temporal-spatial distribution of the traffic flow in the transportation network. In addition, by adjusting the power station exporting power and the refuelling station importing power, the voltage condition of the power system can be improved.

The remainder of this paper is organized as follows. Section II describes the problem formulation. Section III presents the proposed solution. Section IV presents the simulation results. Finally, Section V concludes the paper.

II. Problem Formulation

In this section, different models are presented, including HFCEV refuelling through real-world transportation networks, real-time simulation of the coupled transportation network and power network, hydrogen based microgrid operation model, renewable energy based power station operation model, and utility grid operation model.

A. Hydrogen Vehicle Refuelling Through Real-World Transportation Network

In this section, HFCEV refuelling behavior through real-world transportation networks are presented. A real-world transportation network located in E : 113.93, N : 22.57, Shenzhen, China is studied. The hydrogen vehicles choose the best refuelling station based on the travelling distance and the hydrogen retailing price.

Assume there are N refuelling stations, in each i station, there is a hydrogen refuelling price Pr_i. For each HFCEV, it chooses refuelling station based on the following two rules: (1) the three nearest refuelling stations among N refuelling stations based on distance are firstly selected, i.e., $Dis_{near} = \{D_{near1}, D_{near2}, D_{near3}\}$; (2) then it compares the refuelling price in these three stations, and selects the cheapest price station.

After all HFCEVs select their refuelling stations, vehicles begin travelling through the real-world transportation network. And we monitor the traffic congestion near the N refuelling stations. If the traffic congestion near i station is large, then the i station should increase the price Pr_i to dis-attract vehicles.

In conclusion, the relationship between refuelling hydrogen price and traffic congestion can be seen in the following Fig. 4.

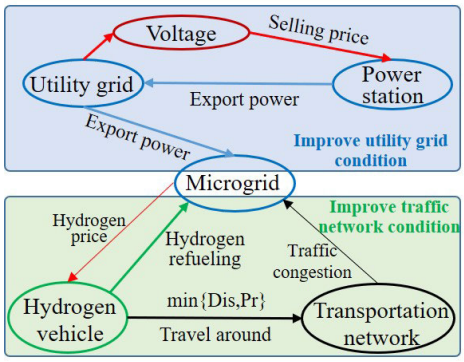

Fig. 4. The relationship between refuelling hydrogen price and the traffic congestion.

In addition, the power station adjusts its exporting power based on the utility grid voltage to improve the utility grid operation condition.

Here, the SUMO traffic simulator is adopted to model the travelling of the HFCEVs. The traffic calculation in SUMO can be described in Fig. 5.

In the SUMO simulator, firstly, upload the graph representation of the real-world transportation network, and the network parameters. Then, set the traffic flow dataset (origin-destination OD flow). After that, use the Depth First Search (DFS) algorithm to find all paths for OD flow. DFS algorithm is often used to search a graph or tree data structure [30]. Then, based on all paths for OD flows, use the Franke-Wolfe algorithm [31] to calculate the traffic flow assignment.

The traffic flow assignment [32] problem can be described as follows.

$$
\begin{aligned}
&min \sum_{\alpha} \int_0^{f_\alpha^t} \tau_\alpha^t(\theta) d\theta \\
&s.t. \sum_{K_{uw}} \varrho_{uw,k}^t = d_{uw}^t \\
&\sum_{uw \in O} \sum_{k \in K_{uw}} \delta_{uw,k,\alpha} \varrho_{uw,k}^t = f_\alpha^t \\
&\varrho_{uw,k}^t > 0
\end{aligned} \tag{1}
$$

$\delta_{uw,k,\alpha}$ is the link-route indicator variable, i.e., if route $k \in K_{uw}$ uses link α, $\delta_{uw,k,\alpha} = 1$, and $\varrho_{uw,k}^t$ is the total traffic flow on route k. $d_{u,w}^t$ is the traffic demand between an origin-destination (OD) pair $u-w$ during time t. $K_{u,w}$ are the routes that connect u, w, O is the set of OD pairs. The travelling time on road α at hour t is $\tau_\alpha^t(f_\alpha^t)$, and is related to the traffic flow f_α^t on road α. The widely used Bureau of Public Roads (BPR) function [32] is adopted to describe the relationship between travelling time and traffic flow: $\tau_\alpha^t(f_\alpha^t) = \tau_\alpha^0 \lfloor 1 + 0.15(\frac{f_\alpha^t}{f_\alpha})^4 \rfloor$. τ_α^0 is the travel time on link α without any congestions and f_α is the link road capacity.

Based on the above traffic flow assignment results, the traffic congestion TC can be calculated. In addition, the refuelling of hydrogen Hy in each station is also calculated, which is transferred to the microgrid operation.

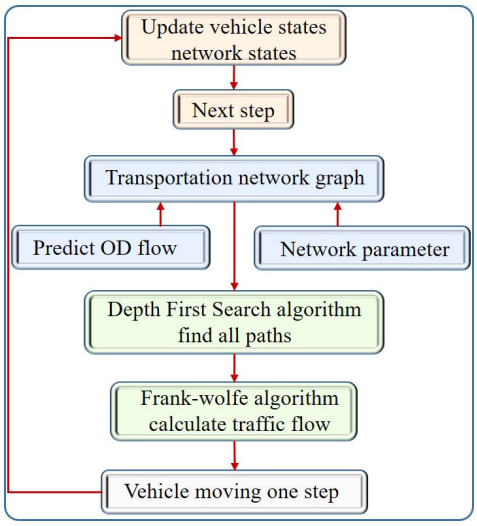

Fig. 5. The traffic calculation in SUMO.

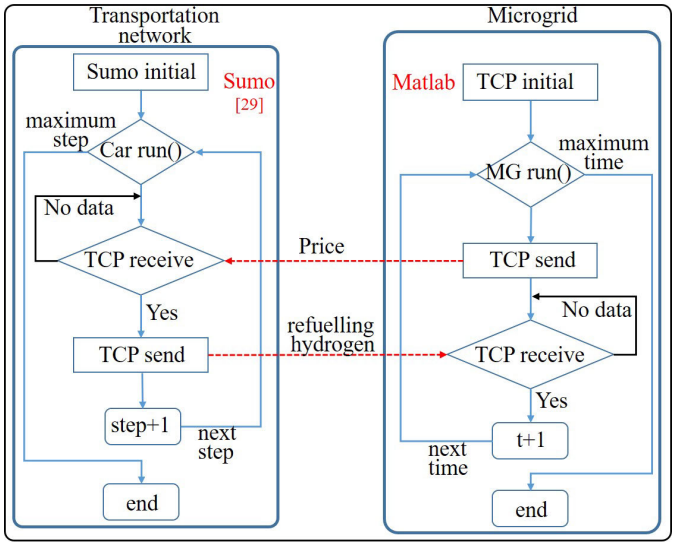

Fig. 6. Tcp/ip send-receive message handling logistic algorithm.

B. Real-Time Simulation for the Coupling of Transportation Network and Power Network

In the above section, the refuelling hydrogen $Hy(t)$ is calculated in Sumo software. However, the microgrid operation problem is developed in Matlab software. Thus, a real-time communication platform to link Sumo and Matlab is needed. In this paper, the tcp/ip message is adopted to exchange information between Sumo and Matlab in real time.

The tcp/ip send-receive message handling logistic algorithm is developed, and presented in Fig. 6.

First, in the Sumo, the "$TCP\_receive$" thread waits to receive the message ($Price$) from Matlab, after it receives the message (through tcp/ip channel), the HFCEVs travel forward one step to the selected destination hydrogen refuelling station. After that, Sumo sends the message (hydrogen refuelling message, traffic congestion message) of each station to Matlab (through tcp/ip channel), and Sumo runs to the next step.

At the same time, in Matlab, the "$TCP\_receive$" thread waits to receive the message (hydrogen refuelling message, traffic congestion message) from Sumo, after it receives the message (through tcp/ip channel), microgrid operation is running for one time step. After that, Matlab sends the message ($Price$) to Sumo (through tcp/ip channel), and Matlab goes to the next time step.

C. Hydrogen Based Microgrid Operation

Based on the above tcp/ip send-receive message handling logistic algorithm, the traffic congestion TC and the refuelling of hydrogen Hy in each station (calculated in Sumo) are then successfully transferred to the microgrid operation problem (developed in Matlab). In the microgrid, hydrogen is produced to cover the refuelling hydrogen demands.

The hydrogen based microgrid is presented in Fig. 1. The installed renewable energy and the utility grid are deployed to produce hydrogen to refuel HFCEVs to cover the refuelling demands Hy.

The operation goal of the microgrid is to minimize the operation cost. The utilization cost of the battery and the hydrogen storage is adopted to decide the dispatching priority of each device. The objective function is represented as:

$$C_{op} = \sum_{t=1}^{T} (B_{cost}^{ch}(t) + B_{cost}^{dis}(t) + H_{cost}^{ele}(t) + H_{cost}^{fc}(t) + \gamma \cdot Ug(t) + \alpha \cdot P_{LS}(t) + \beta \cdot P_{curt}(t)) \quad (2)$$

$$B_{cost}^{ch,dis}(t) = \frac{C_{bat}^{inv} \cdot P_{ch,dis}(t) \cdot \eta_b}{2 \cdot N_{bat}} \quad (3)$$

$$H_{cost}^{ele,fc}(t) = \left(\frac{C_{ele,fc}^{inv}}{N_{ele,fc}} + C_{ele,fc}^{o\&m} \right) \cdot \delta_{ele,fc}(t) + C_{ele,fc}^{start} \cdot \Delta\delta_{ele,fc}(t) \quad (4)$$

where $Ug(t)$ is the power from utility grids, γ is the coefficient. $P_{LS}(t)$ is the shedding loads, $P_{curt}(t)$ is the curtailed renewable generations output, and α and β are the penalty values. C_{bat}^{inv} is the investment cost for the battery storage, and N_{bat} is the number of cycles over its lifetime. $C_{ele,fc}^{inv}$ are the investment costs of the electrolyzer and the fuel cell. $C_{ele,fc}^{o\&m}$ are the operation and maintenance costs. $C_{ele,fc}^{start}$ are the startup cost. $N_{ele,fc}$ represents the lifetime of the electrolyzer and fuel cell. $\delta_{ele,fc}(t)$ describe their state (i.e., 1 for on, 0 for off). Finally, $\Delta\delta_i$ represents whether the unit is starting or not, and is defined as:

$$\Delta\delta_i(t) = \max\{\delta_i(t) - \delta_i(t-1), 0\}, i = \{ele, fc\} \quad (5)$$

The above optimization problem is subject to several constraints.

$$\delta_j(t) \cdot P_j^{min} \le Z_j(t) = \delta_j(t) \cdot P_j(t) \le \delta_j(t) \cdot P_j^{\max}$$
$$j = \{ele, fc, ch, disch\} \quad (6)$$

$$\delta_{ele}(t) + \delta_{fc}(t) \le 1 \quad (7)$$

$$\delta_{ch}(t) + \delta_{disch}(t) \le 1 \quad (8)$$

$$\begin{cases} SOC(t) = SOC(t-1) \\ +\dfrac{P_{ch}(t)\cdot\Delta t\cdot\eta_{ch} - P_{dis}(t)\cdot\Delta t\cdot\eta_{dis}}{Ca_{ba}} \\ SOC_{min} \le SOC(t) \le SOC_{max} \end{cases} \tag{9}$$

$$\begin{cases} LOH(t) = LOH(t-1) + \dot{n}_{H2}^{pro}\Delta t - \dot{n}_{H2}^{con}\Delta t \\ -\mathbf{Hy(t)} \\ \dot{n}_{H2}^{pro} = f_{ele}(Z_{ele}), \dot{n}_{H2}^{con} = f_{fc}(Z_{fc}) \\ LOH_{min} \le LOH(t) \le LOH_{\max} \end{cases} \tag{10}$$

$$\begin{cases} \Delta\delta_i(t) = \delta_i(t)\cdot(1-\delta_i(t-1)), i = \{ele, fc\} \\ -\delta_i(t) + \Delta\delta_i(t) \le 0 \\ -(1-\delta_i(t-1)) + \Delta\delta_i(t) \le 0 \\ \delta_i(t) + (1-\delta_i(t-1)) - \Delta\delta_i(t) \le 1 \end{cases} \tag{11}$$

$$\begin{aligned} &Ug(t) + P_{RES}(t) - P_{curt}(t) - Z_{ele}(t) + Z_{fc}(t) \\ &\quad - Z_{ch}(t) + Z_{dis}(t) = (P_{load}(t) - P_{LS}(t)) \end{aligned} \tag{12}$$

Constraint (6) describes the outputs that have been limited to the minimum and maximum values. Constraint (7) describes the electrolyzer and the fuel cell can not work at the same time. Constraint (8) describes the battery cannot charge and discharge at the same time. Constraints (9), (10) describe the limitation of the state of charge and the level of hydrogen. Constraint (11) rewrite equation (5), and transform the non-linear equation in linear equations. Constraint (12) describes the power balance between generation and demand, P_{RES} is the renewable energy output.

Based on the above objective function and constraints, the microgrid operation problem can be summarized as follows:

$$\min_{z,Ug}\{C_{\text{op}}\} \quad \text{s.t. } (6)-(12) \tag{13}$$

where z is the set of decision variables, Ug is the imported power from power network.

D. Operation of the Renewable Energy Based Power Station

The operation of the renewable energy based power station is similar to microgrids. The objective function is presented as follows:

$$\begin{aligned} C_{op}^{ps} = \sum_{t=1}^{T}(&B_{cost}^{ch}(t) + B_{cost}^{dis}(t) + H_{cost}^{ele}(t) + H_{cost}^{fc}(t) \\ &+ Pr_{selling}\cdot P_{export}(t) + \beta\cdot P_{curt}(t)) \end{aligned} \tag{14}$$

where $Pr_{selling}$ is the energy selling price, which is adjusted based on the utility grid voltage, and P_{export} is the exported power of the power station.

For the power station, it supplies renewable energy to the utility grid, and it always exports energy P_{export}. Thus, the constraint (12) should be revised as follows:

$$\begin{aligned} &P_{RES}(t) - P_{curt}(t) - Z_{ele}(t) + Z_{fc}(t) \\ &\quad - Z_{ch}(t) + Z_{dis}(t) = (P_{load}(t) + P_{export}(t)) \end{aligned} \tag{15}$$

The renewable energy based power station operation problem can be summarized as follows:

$$\min_{u,P_{export}}\{C_{\text{op}}^{ps}\} \quad \text{s.t. } (6)-(11), (15) \tag{16}$$

where u is the set of decision variable, P_{export} is the exported power to utility grid.

E. Operation of the Utility Grid

Microgrid imports power from utility grid $Ug(t)$, and power station exports power to utility grid $P_{export}(t)$. For the utility grid operation, it is an optimal power flow (OPF) problem. The OPF problem can be represented as follows:

$$\min_{P_g,Q_g,V} C_{ug} = \sum_{i=1}^{n_g}\left\{f_P^i(P_g^i) + f_Q^i(Q_g^i)\right\} \tag{17}$$

$$\begin{aligned} s.t. \quad & P_i^g + \mathbf{P_{export,i}} = P_i^{load} \\ & + \sum_{j=1}^{n_{bus}} V_i V_j (G_{ij}^{line} cos\theta_{ij} + B_{ij}^{line} sin\theta_{ij}) \\ & + \mathbf{Ug_i} \end{aligned}$$

$$Q_i^g = Q_i^{load} + \sum_{j=1}^{n_{bus}} V_i V_j (G_{ij}^{line} sin\theta_{ij} - B_{ij}^{line} cos\theta_{ij}) \tag{18}$$

$$\begin{aligned} &V_m^{i,min} \le V_m^i \le V_m^{i,max}; i = 1,2,\ldots,n_{bus} \\ &P_g^{i,min} \le P_g^i \le P_g^{i,max}; i = 1,2,\ldots,n_g \\ &Q_g^{i,min} \le Q_g^i \le Q_g^{i,max}; i = 1,2,\ldots,n_g \end{aligned} \tag{19}$$

where the P_g^i, Q_g^i are the real and reactive power of the i^{th} generator. f_P^i, f_Q^i are the individual polynomial cost function of the i^{th} generator. P_i^{load}, Q_i^{load} are the real and reactive load demand at bus i. $P_{export,i}$ is the power station real exported power to utility grid at bus i. Ug_i is the real exported power to microgrids at bus i. $G_{ij}^{line}, B_{ij}^{line}$ are the parameters of the power lines from bus i to bus j. $V_m^i, V_m^{i,min}, V_m^{i,max}$ are the voltage magnitude, minimum voltage magnitude, and maximum voltage magnitude at bus i. $P_g^{i,min}, P_g^{i,max}, Q_g^{i,min}, Q_g^{i,max}$ are the minimum and maximum real and reactive power of i generator.

F. The Whole Problem Formulation

In conclusion, the whole problem formulation can be represented as follows:

In the Sumo simulator, based on the received price Pr, HFCEVs travel to the selected refuelling station to refuel hydrogen, and one can calculate the refuelling hydrogen amount in each station Hy, and the traffic congestion near each station TC.

$$\{Hy, TC\} = SUMO(Pr, Vehicles) \tag{20}$$

Then, based on the received refuelling hydrogen Hy, microgrids run their operation strategy, and one can calculate the scheduling results and the imported power from the utility grid Ug. In addition, based on the received traffic congestion information TC and the utility grid voltage V, the microgrid can update the hydrogen price Pr.

$$\begin{cases} Ug = arg\min_{z,Ug}\{C_{\text{op}}(Hy)\} \\ Pr = f(TC, V) \end{cases} \tag{21}$$

Based on the selling price $Pr_{selling}$, the power station runs its operation problem, and one can obtain the exported power to the utility grid P_{export}. In addition, the selling price

Algorithm 1 The Proposed Coupling Power Network and Transportation Network Sequential Algorithm

for

do TCP/IP: $Matlab$: $Pr_t \rightarrow tcp/ip \rightarrow Sumo$;

Sumo: Update the hydrogen price $\overset{\rightsquigarrow\rightsquigarrow}{Pr}_t$;

Sumo: Solve $\{Hy_t, TC_t\} = SUMO(Pr_t, Vehicles_t)$;
Sumo outputs: $\{Hy_t, TC_t\}$

TCP/IP: $Sumo$: $\{Hy_t, TC_t\} \rightarrow tcp/ip \rightarrow Matlab$;

Matlab: Solve $Ug_t = arg \min_{z_t, Ug_t} \{\overset{\rightsquigarrow\rightsquigarrow}{C}_{\text{op}}(Hy_t)\}$;
Call Gurobi:

$$\min_{z, Ug_t} \{C_{\text{op}}\} \quad \text{s.t. (6)} - \text{(12)}$$

Matlab: Solve $P_{export,t} = arg \min_{u_t, P_{export,t}} \{C^{ps}_{\text{op}}(Pr_{selling,t})\}$;
Call Gurobi:

$$\min_{u, P_{export,t}} \{C^{ps}_{\text{op}}\} \quad \text{s.t. (6)} - \text{(11), (15)}$$

Matlab: Solve $(P_t, Q_t, V_t) = arg \min_{P_{g,t}, Q_{g,t}, V_t} C_{ug}(Ug_t, P_{export,t})$;
Call Matpower:

$$\min_{P_g, Q_g, V} \{C_{ug}\} \quad \text{s.t. (18)} - \text{(19)}$$

Matlab: Calculate the new price $Pr_{t+1} = f(TC_t, V_t)$, $Pr_{selling,t+1} = g(V_t)$ for next time $t+1$;

t=t+1;

end for

$Pr_{selling}$ is dynamically updated based on the utility grid voltage V.

$$\begin{cases} P_{export} = arg \min_{u, P_{export}} \{C^{ps}_{\text{op}}(Pr_{selling})\} \\ Pr_{selling} = g(V) \end{cases} \tag{22}$$

After that, based on the microgrid imported power Ug and power station exported power P_{export}, utility grid runs its optimal power flow problem, and check the voltage variation.

$$(P, Q, V) = arg \min_{P_g, Q_g, V} C_{ug}(Ug, P_{export}) \tag{23}$$

III. The Proposed Solution

The above problem is a coupled complex optimization problem. Fortunately, it can be solved sequentially. First, solve the HFCEV refuelling within the transportation network problem in SUMO. Second, solve the refuelling station microgrid operation problem in Matlab. It is a mixed integer programming optimization and is solved by Gurobi [33]. Third, solve the power station operation problem, which is also solved by Gurobi. Forth, solve the power grid OPF problem by Matpower [34]. Last, update the power station selling price and the refuelling station hydrogen price. Repeat the above sequential steps until the stopping criteria are satisfied. The solving algorithm is presented in Algorithm 1.

f is the hydrogen price adjusting strategy: (1) if TC_t is high, increase Pr_{t+1} to dis-attract HFCEV refuelling, else if TC_t is low, decrease Pr_{t+1} to attract HFCEV refuelling; (2) if V_t is high, decrease Pr_{t+1} to attract HFCEV refuelling; else if V_t is low, increase Pr_{t+1} to dis-attract HFCEV refuelling.

g is the power station selling price adjusting strategy: if V_t is high, decrease $Pr_{selling,t+1}$ to decrease selling profits to decrease output power; else if V_t is low, increase $Pr_{selling,t+1}$ to increase selling profits to increase output power.

IV. Simulation Results

In this section, four different coupled structures are deployed, which are presented in Fig. 7. Case 1 and Case 2 are implemented to compare the impact of the power station on the coupled network. Case 2 and Case 3 are deployed to compare the impact of the price strategy on the coupled transportation network and power system. Case 3 and Case 4 are implemented to compare the impact of the smart LSTM [35] price decision strategy on the coupled network. Four structures are summarized as follows:

1) In Case 1, the power station is not considered, only microgrids are considered;
2) In Case 2, the power station is considered, the exporting power of the power station is adjusted based on the selling price, and the selling price is adjusted based on the utility grid voltage; in addition, in microgrid, the hydrogen price is adjusted based on the traffic congestion;
3) In Case 3, the power station is considered, the difference is that in the microgrid, the hydrogen price is adjusted based on the utility grid voltage and the traffic congestion;
4) In Case 4, an LSTM network is adopted to train the relationship between states (voltage, traffic flow) and the price. The hydrogen price is decided based on the smart LSTM network.

A. Simulation Results for Case 1

In Case 1 (Fig. 7), the power station is not considered, and three different scenarios Case 1A, Case 1B, and Case 1C are implemented to compare the impact of price. In addition, in order to study the users' behaviors impacts, three different users' behaviors in Case 1C are further compared.

- In scenario Case 1A, hydrogen price is not considered, and vehicles choose the nearest distance station to refuel hydrogen;
- In scenario Case 1B, fixed hydrogen price is considered;
- In scenario Case 1C, dynamic hydrogen price is considered, and the price is dynamically adjusted based on the traffic congestion. Three different users choosing refuelling station strategies are compared.
  - Case 1C-user-S1: users choose a station based on the following two rules: (1) the three nearest refuelling stations are firstly selected based on distance, $Dis_{near} = \{D_{near1}, D_{near2}, D_{near3}\}$; (2) then it compares the refuelling price in these three stations, and selects the cheapest price station.

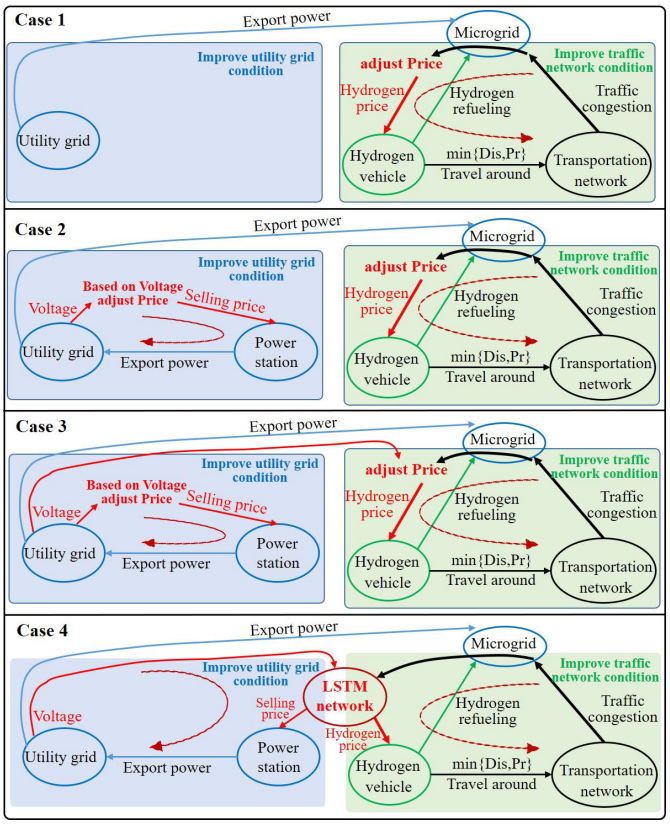

Fig. 7. The simulation structure for case 1, case 2, case 3, and case 4.

- Case 1C-user-S2: users have 50% probability to select strategy user-S1, and the other probability to select a random station from the three nearest stations $Dis_{near} = \{D_{near1}, D_{near2}, D_{near3}\}$.
- Case 1C-user-S3: users have 50% probability to select strategy user-S1, and the other probability to select the nearest station D_{near1}.

Four microgrids are considered to produce hydrogen to refuel HFCEVs. The IEEE 30-node network is considered as the utility grid.

The refuelling hydrogen in each station is presented in Fig. 8. Every 200 seconds, each station updates the hydrogen price, and HFCEVs receive the new price, and choose the appropriate refuelling station to refuel hydrogen. It can be seen that with different hydrogen price strategies, the refuelling hydrogen in each station is different.

The relationship between the dynamic price and the traffic flow is presented in Fig. 9. It can be seen that when the traffic flow is high, the price is then adjusted higher to disattract vehicles to refuel hydrogen. When the traffic is low, the price is adjusted lower to attract vehicles to charge hydrogen.

The states of the transportation network under different scenarios are presented in Tab. I. It can be seen that in Case 1B (fixed price), the waiting time is reduced by 13.51%, and the time loss is reduced by 9.22%. It can be seen that in Case 1C-user-S1 (dynamic price), the traffic congestion of the transportation network is further improved, the waiting time is further reduced by 17.71%, and the time loss of the network is further reduced by 13.29%. In Case 1C-user-S2, users' behaviors have negative impacts on the traffic congestion of the transportation network and increase the waiting time. In Case 1C-user-S3, the conditions of the transportation network are improved, but the improvements are not better than that in Case 1C-user-S1.

The operation costs of four microgrids are presented in Fig. 10. It can be seen that with three different price strategies, the microgrid operation costs are different, this is because that refuelling hydrogen in each microgrid is different. The level of hydrogen (LOH) and state of charge (SOC) in four microgrids are presented in Figs. 11, 12. The produced hydrogen is supplied to refuel vehicles. It can be seen that in Case 1A

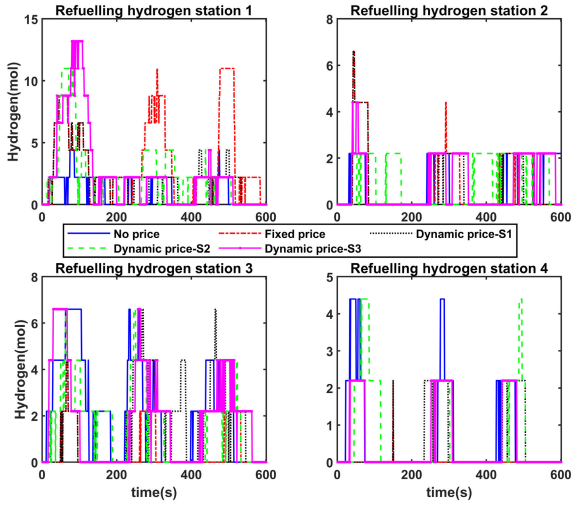

Fig. 8. The refuelling hydrogen in four stations for case 1.

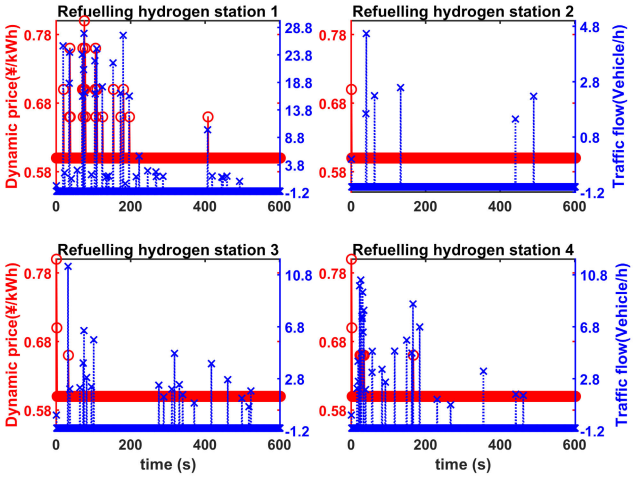

Fig. 9. The relationship between the dynamic price and the traffic flow for case 1.

TABLE I
THE STATES OF THE TRANSPORTATION NETWORK FOR CASE 1

Cases	duration (s)	waiting time (s)	time loss (s)	waiting time reduced by	time loss reduced by
Case1A	1294.64	849.56	1074.15	–	–
Case1B	1194.88	734.77	975.08	13.51%	9.22%
Case1C-user-S1	1148.97	699.14	931.43	17.71%	13.29%
Case1C-user-S2	1321.05	868.77	1097.72	−2.26%	−2.19%
Case1C-user-S3	1221.05	771.25	999.66	9.22%	6.93%

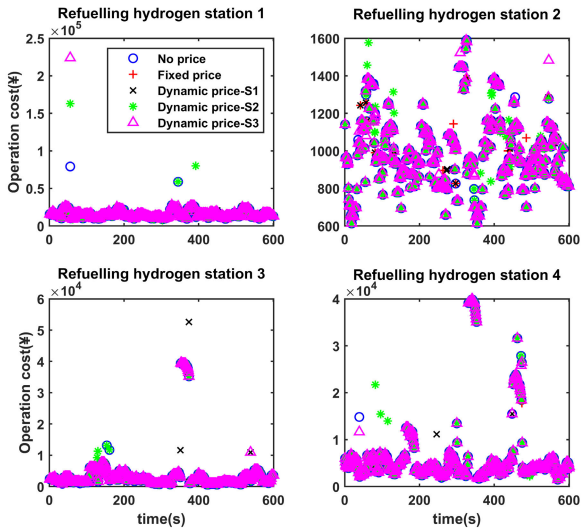

Fig. 10. The operation cost of four microgrids for case 1.

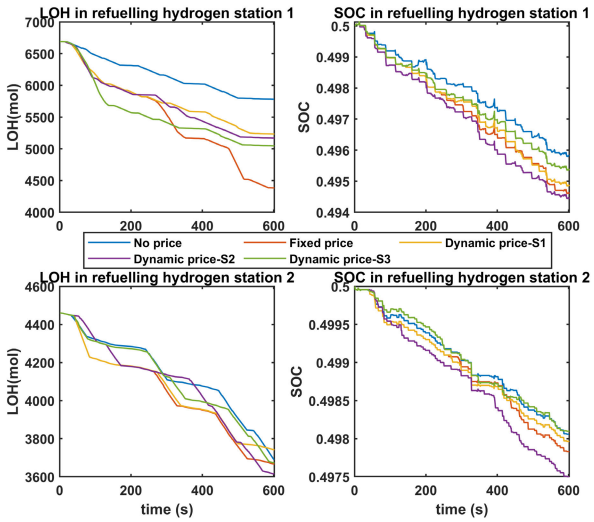

Fig. 11. The LOH and SOC in microgrid 1 and microgrid 2 for case 1.

(no price), the charging hydrogen in station 1 and station 2 are smaller than that in station 3 and station 4 (because LOH and SOC curves in station 1 and station 2 have decreased smoothness). In Case 1B and Case 1C, the charging hydrogen in station 3 and station 4 are smaller than that in station 1 and station 2 (because LOH and SOC curves in station 3 and station 4 are decreased smoothness). This is because, with the guidance of the price, vehicles choose the cheapest station to refuel hydrogen.

The voltage deviation of the IEEE 30-node network is presented in Fig. 13. The voltage deviation has not unit and is defined as $\sum_{k=1}^{n}(\frac{V_k^{ref}-V_k}{V_k^{ref}})^2$, V_k^{ref} is the reference voltage 1, V_k is the k node voltage. It can be seen that the voltage deviations are all within the security bound. This means that the utility grid operates safely to export power to microgrids.

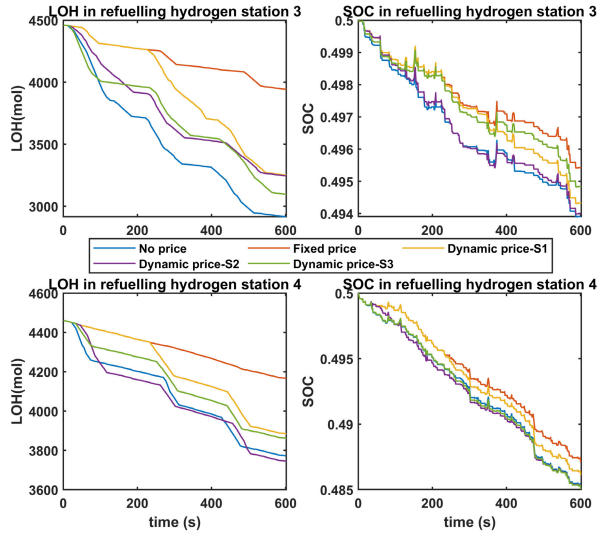

Fig. 12. The LOH and SOC in microgrid 3 and microgrid 4 for case 1.

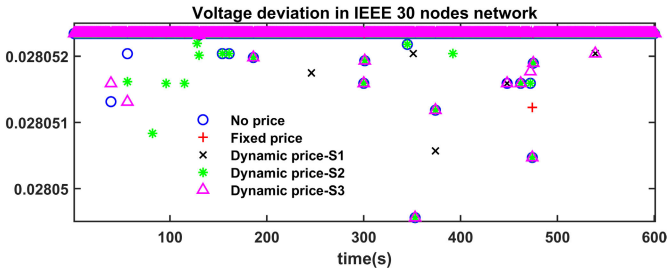

Fig. 13. The voltage deviation of the IEEE 30-node network for case 1.

B. Simulation Results for Case 2

In Case 2 (Fig. 7), a power station is considered. In a power station, the exporting power is adjusted based on the selling price, and the selling price is adjusted based on the utility grid voltage. One can adjust the voltage of the utility grid by adjusting the exporting power of the power station, and at last, improve the operation condition of the utility grid.

The voltage v.s. dynamic price v.s. power output in the power station is presented in Fig. 14. It can be seen that when the voltage increases (decreases), the selling price decreases (increases); when the selling price decreases (increases), the exporting power of the power station decreases (increases); when the exporting power of the power station decreases (increases), the voltage decreases (increases). The voltage condition of the utility grid can be improved by adjusting the output power of the power station.

The voltage deviation of the IEEE 30-node network for Case 2 is presented in Fig. 15. It can be seen that in Case 2 (green colour), the voltage deviation of the IEEE 30-node network is smaller than that in Case 1. It reveals that by installing the power station, one can improve the voltage condition of the utility grid network.

In addition, the dynamic hydrogen price strategy can guide the vehicles refuelling and improve the traffic congestion of the transportation network. The states of the transportation network for Case 2 are the same as that in Case1C (Tab. I),

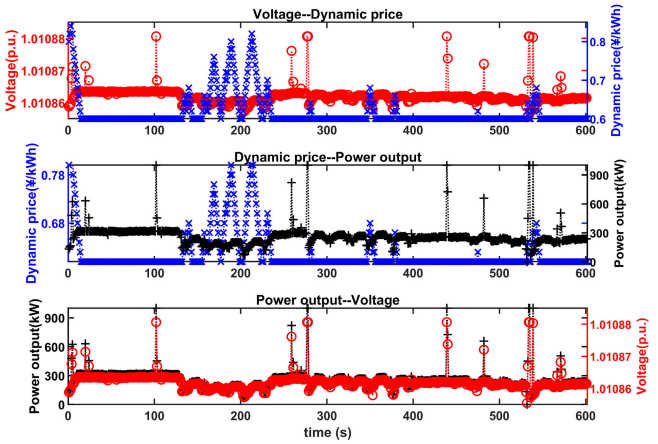

Fig. 14. Voltage v.s. dynamic price v.s. power output in power station for case 2.

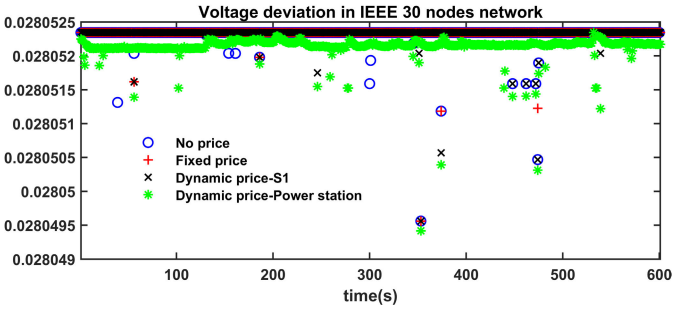

Fig. 15. The voltage deviation of the IEEE 30-node network for case 2 (named as "dynamic price-power station" in the figure).

because the hydrogen price updating strategy is the same as in Case1C-user-S1.

C. Simulation Results for Case 3

In Case 3 (Fig. 7), a power station is considered, the difference is that in the microgrid, the hydrogen price is adjusted based on the utility grid voltage and the traffic congestion.

The voltage deviation of the IEEE 30-node network for Case 3 is presented in Fig. 16. It can be seen that in Case 3 (pink colour), the voltage deviation of the IEEE 30-node network is almost the same as that in Case 2. It shows that by adjusting the exporting power of the power station and the importing power of the refuelling station microgrids at the same time, the utility grid voltage condition can be further improved.

The states of the transportation network for Case 3 are presented in Tab. II. It can be seen that in Case 3, the waiting time is reduced by 16.03%, and the time loss is reduced by 11.62%. However, the reduced values are smaller than that in Case1C-user-S1, this is because in Case 3, the hydrogen price is adjusted based on the utility grid voltage and the traffic congestion at the same time, and traffic congestion is not the only consideration, which makes the adjustment of the hydrogen price to the traffic flow even weaker. Thus, the price guidance of the vehicles to improve traffic congestion is worse than Case1C-user-S1, then the improvement of the

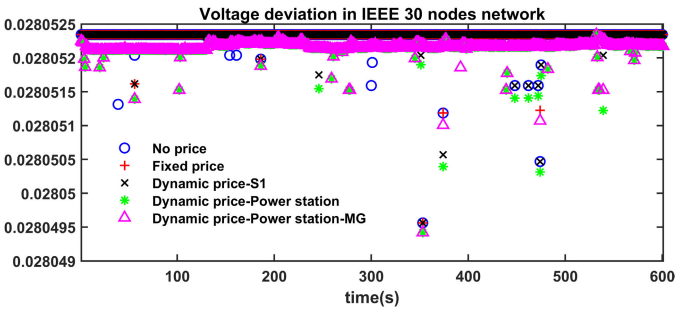

Fig. 16. The voltage deviation of the IEEE 30-node network for case 3 (named as "dynamic price-power station-MG" in the figure).

TABLE II

THE STATES OF THE TRANSPORTATION NETWORK FOR CASE 3

Cases	duration (s)	waiting time (s)	time loss (s)	waiting time reduced by	time loss reduced by
Case1C-user-S1	1148.97	699.14	931.43	17.71%	13.29%
Case3	1168.31	713.36	949.33	16.03%	11.62%

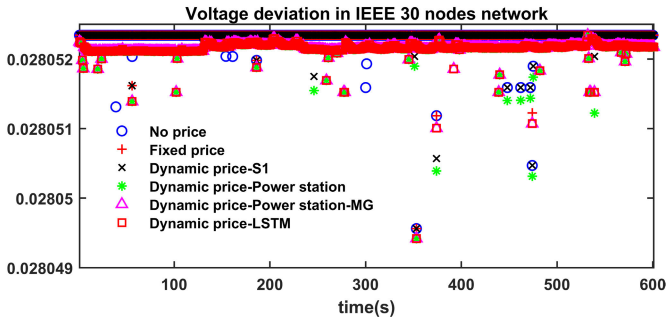

Fig. 17. The voltage deviation of the IEEE 30-node network for case 4 (named as "dynamic price-LSTM" in the figure).

TABLE III

THE STATES OF THE TRANSPORTATION NETWORK FOR CASE 4

Cases	duration (s)	waiting time (s)	time loss (s)	waiting time reduced by	time loss reduced by
Case1C-user-S1	1148.97	699.14	931.43	17.71%	13.29%
Case3	1168.31	713.36	949.33	16.03%	11.62%
Case4	1187.72	722.68	962.07	14.93%	10.43%

traffic congestion of the transportation network is smaller than Case1C-user-S1.

D. Simulation Results for Case 4

In Case 4 (Fig. 7), an LSTM network is adopted to train the relationship between states (voltage, traffic flow) and the price. Then, the trained LSTM network is deployed to adjust the hydrogen price.

The voltage deviation of the IEEE 30-node network for Case 4 is presented in Fig. 17. It can be seen that in Case 4 (red square), the voltage deviation of the IEEE 30-node network is almost the same as that in Case 3. It reveals that by finding the mapping function between voltage/traffic flow and price, and then adjusting the price through the mapping function, the utility grid voltage condition can be improved effectively.

The states of the transportation network for Case 4 are presented in Tab. III. It can be seen that in Case 4, the waiting time is reduced by 14.93%, and the time loss is

reduced by 10.43%. However, the reduced values are smaller than that in Case 3, this is because in Case 4, the hydrogen price is adjusted based on the trained LSTM network, and the performance of the LSTM is mainly decided by the original history dataset, thus the LSTM network should be carefully designed.

V. Conclusion

In this paper, we focus on studying the real-time hydrogen refuelling of HFCEV through the coupled transportation network and power system. A Sumo simulator is deployed to model the HFCEV refuelling hydrogen. The hydrogen refuelling station is modeled as a microgrid and aims to minimize its operation cost. An IEEE 30-node network is adopted to export energy to microgrids to produce hydrogen. Renewable energy based power station is deployed to supply renewable energy to the utility grid. At last, four different coupled structures are deployed, and different HFCEV refuelling strategies are compared.

Based on the above simulation results, some conclusions can be concluded as follows: 1) with the dynamic hydrogen price, the congestion of the transportation network is improved, the waiting time is reduced by 17.71%, and time loss of the network is reduced by 13.29%; 2) users' behavior choosing strategy has a big influence on the transportation network; 3) based on the long short-term memory network smart decision strategy, the congestion of the transportation network is improved, but the training performance should be carefully designed.

The results demonstrate that by adjusting the hydrogen price, the traffic congestion of the transportation network can be improved, and by adjusting the power station exporting power and the refuelling station importing power, the voltage condition of the utility grid can be improved.

References

[1] *Co2 Emissions in 2022*, License: CC BY 4.0, IEA, Paris, 2022. [Online]. Available: https://www.iea.org/reports/co2-emissions-in-2022

[2] A. Ajanovic and R. Haas, "Prospects and impediments for hydrogen and fuel cell vehicles in the transport sector," *Int. J. Hydrogen Energy*, vol. 46, no. 16, pp. 10049–10058, Mar. 2021.

[3] M. Fayyazi et al., "Artificial intelligence/machine learning in energy management systems, control, and optimization of hydrogen fuel cell vehicles," *Sustainability*, vol. 15, no. 6, p. 5249, 2023. [Online]. Available: https://www.mdpi.com/2071-1050/15/6/5249

[4] A. Murugan et al., "Measurement challenges for hydrogen vehicles," *Int. J. Hydrogen Energy*, vol. 44, no. 35, pp. 19326–19333, Jul. 2019.

[5] K. Reddi, A. Elgowainy, N. Rustagi, and E. Gupta, "Impact of hydrogen SAE J2601 fueling methods on fueling time of light-duty fuel cell electric vehicles," *Int. J. Hydrogen Energy*, vol. 42, no. 26, pp. 16675–16685, Jun. 2017.

[6] H. Kim, M. Eom, and B.-I. Kim, "Development of strategic hydrogen refueling station deployment plan for Korea," *Int. J. Hydrogen Energy*, vol. 45, no. 38, pp. 19900–19911, Jul. 2020.

[7] Y. Gu, Q. Chen, J. Xue, Z. Tang, Y. Sun, and Q. Wu, "Comparative techno-economic study of solar energy integrated hydrogen supply pathways for hydrogen refueling stations in China," *Energy Convers. Manage.*, vol. 223, Nov. 2020, Art. no. 113240.

[8] N. Chrysochoidis-Antsos, M. R. Escudé, and A. J. M. van Wijk, "Technical potential of on-site wind powered hydrogen producing refuelling stations in The Netherlands," *Int. J. Hydrogen Energy*, vol. 45, no. 46, pp. 25096–25108, Sep. 2020.

[9] B. Li, H. Miao, and J. Li, "Multiple hydrogen-based hybrid storage systems operation for microgrids: A combined TOPSIS and model predictive control methodology," *Appl. Energy*, vol. 283, Feb. 2021, Art. no. 116303.

[10] R. S. El-Emam and H. Özcan, "Comprehensive review on the techno-economics of sustainable large-scale clean hydrogen production," *J. Cleaner Prod.*, vol. 220, pp. 593–609, May 2019.

[11] J.-J. Hwang, "Sustainability study of hydrogen pathways for fuel cell vehicle applications," *Renew. Sustain. Energy Rev.*, vol. 19, pp. 220–229, Mar. 2013.

[12] S. Nistor, S. Dave, Z. Fan, and M. Sooriyabandara, "Technical and economic analysis of hydrogen refuelling," *Appl. Energy*, vol. 167, pp. 211–220, Apr. 2016.

[13] L. Zhao and J. Brouwer, "Dynamic operation and feasibility study of a self-sustainable hydrogen fueling station using renewable energy sources," *Int. J. Hydrogen Energy*, vol. 40, no. 10, pp. 3822–3837, Mar. 2015.

[14] S. Carr, F. Zhang, F. Liu, Z. Du, and J. Maddy, "Optimal operation of a hydrogen refuelling station combined with wind power in the electricity market," *Int. J. Hydrogen Energy*, vol. 41, no. 46, pp. 21057–21066, Dec. 2016.

[15] M. Kiaee, A. Cruden, P. Chladek, and D. Infield, "Demonstration of the operation and performance of a pressurised alkaline electrolyser operating in the hydrogen fuelling station in Porsgrunn, Norway," *Energy Convers. Manage.*, vol. 94, pp. 40–50, Apr. 2015.

[16] J. Alazemi and J. Andrews, "Automotive hydrogen fuelling stations: An international review," *Renew. Sustain. Energy Rev.*, vol. 48, pp. 483–499, Aug. 2015.

[17] W. Wei, L. Wu, J. Wang, and S. Mei, "Expansion planning of urban electrified transportation networks: A mixed-integer convex programming approach," *IEEE Trans. Transport. Electrific.*, vol. 3, no. 1, pp. 210–224, Mar. 2017.

[18] X. Wang, M. Shahidehpour, C. Jiang, and Z. Li, "Coordinated planning strategy for electric vehicle charging stations and coupled traffic-electric networks," *IEEE Trans. Power Syst.*, vol. 34, no. 1, pp. 268–279, Jan. 2019.

[19] W. Wei, S. Mei, L. Wu, M. Shahidehpour, and Y. Fang, "Optimal traffic-power flow in urban electrified transportation networks," *IEEE Trans. Smart Grid*, vol. 8, no. 1, pp. 84–95, Jan. 2017.

[20] W. Wei, S. Mei, L. Wu, J. Wang, and Y. Fang, "Robust operation of distribution networks coupled with urban transportation infrastructures," *IEEE Trans. Power Syst.*, vol. 32, no. 3, pp. 2118–2130, May 2017.

[21] S. Xie, Z. Hu, and J. Wang, "Two-stage robust optimization for expansion planning of active distribution systems coupled with urban transportation networks," *Appl. Energy*, vol. 261, Mar. 2020, Art. no. 114412.

[22] S. Xie, Z. Hu, J. Wang, and Y. Chen, "The optimal planning of smart multi-energy systems incorporating transportation, natural gas and active distribution networks," *Appl. Energy*, vol. 269, Jul. 2020, Art. no. 115006.

[23] Y. Liu, Y. Wang, Y. Li, H. B. Gooi, and H. Xin, "Multi-agent based optimal scheduling and trading for multi-microgrids integrated with urban transportation networks," *IEEE Trans. Power Syst.*, vol. 36, no. 3, pp. 2197–2210, May 2021.

[24] X. Xu et al., "Risk-based scheduling of an off-grid hybrid electricity/hydrogen/gas/ refueling station powered by renewable energy," *J. Cleaner Prod.*, vol. 315, Sep. 2021, Art. no. 128155.

[25] X. Xu et al., "Optimal operational strategy for an offgrid hybrid hydrogen/electricity refueling station powered by solar photovoltaics," *J. Power Sources*, vol. 451, Mar. 2020, Art. no. 227810.

[26] A. Dadkhah, D. Bozalakov, J. D. M. De Kooning, and L. Vandevelde, "On the optimal planning of a hydrogen refuelling station participating in the electricity and balancing markets," *Int. J. Hydrogen Energy*, vol. 46, no. 2, pp. 1488–1500, Jan. 2021.

[27] X. Wu, S. Qi, Z. Wang, C. Duan, X. Wang, and F. Li, "Optimal scheduling for microgrids with hydrogen fueling stations considering uncertainty using data-driven approach," *Appl. Energy*, vol. 253, Nov. 2019, Art. no. 113568.

[28] F. Grüger, L. Dylewski, M. Robinius, and D. Stolten, "Carsharing with fuel cell vehicles: Sizing hydrogen refueling stations based on refueling behavior," *Appl. Energy*, vol. 228, pp. 1540–1549, Oct. 2018.

[29] P. A. Lopez, "Microscopic traffic simulation using sumo," in *Proc. 21st Int. Conf. Intell. Transp. Syst. (ITSC)*, 2018, pp. 2575–2582.

[30] Brilliant Org. (2021). [Online]. Available: https://brilliant.org/wiki/depth-first-search-dfs/

[31] J. Holmgren and P. O. Lindberg, "Upright stiff: Subproblem updating in the FW method for traffic assignment," *EURO J. Transp. Logistics*, vol. 3, no. 3, pp. 205–225, Oct. 2015.
[32] X. Liu, C. B. Soh, T. Zhao, and P. Wang, "Stochastic scheduling of mobile energy storage in coupled distribution and transportation networks for conversion capacity enhancement," *IEEE Trans. Smart Grid*, vol. 12, no. 1, pp. 117–130, Jan. 2021.
[33] (2023). *Gurobi*. [Online]. Available: http://www.gurobi.com/resources/getting-started/mip-basics
[34] (2023). *Matpower*. [Online]. Available: https://matpower.org/
[35] S. Hochreiter and J. Schmidhuber, "Long short-term memory," *Neural Comput.*, vol. 9, no. 8, p, pp. 1735–1780, 1997.

Bei Li (Member, IEEE) received the B.S. and M.Sc. degrees in electrical engineering from Beijing Jiaotong University, Beijing, China, in 2012 and 2015, respectively, and the Ph.D. degree in electrical engineering from Universit Bourgogne Franche-Comt, France, in 2018. From 2015 to 2019, he conducted research with FCLAB, France. Since 2019, he has been an Assistant Professor with the College of Chemistry and Environmental Engineering, Shenzhen University, China. His research interests include hydrogen storage microgrid, energy management strategies, and energy transportation coupled networks.

Jiangchen Li (Member, IEEE) received the B.Eng. degree in electronic science and technology and the M.Sc. degree in microelectronics and solid-state electronics from Huazhong University of Science and Technology, Wuhan, China, in 2011 and 2014, respectively, and the Ph.D. degree in transportation engineering from the University of Alberta, Edmonton, Canada, in 2021. He was a Post-Doctoral Fellow with the Centre for Smart Transportation, Department of Civil and Environmental Engineering, University of Alberta, in 2021, and Tsinghua University in 2023. He is currently an Associate Professor with Nanjing University of Aeronautics and Astronautics. His current research interests include connected and automated traffic flow and transportation systems.

Zhixiong Li (Senior Member, IEEE) received the Ph.D. degree in transportation engineering from Wuhan University of Technology in 2013. He is with the Faculty of Mechanical Engineering, Opole University of Technology, Poland. He is the author/coauthor of two books and over 100 articles. His research interests include dynamic system modeling and optimization and machine learning and applications. He is an Associate Editor of IEEE TRANSACTIONS ON INTELLIGENT TRANSPORTATION SYSTEMS and a Column Editor of *IEEE Intelligent Transportation Systems Magazine*.

Miguel Angel Sotelo (Fellow, IEEE) received the Ph.D. degree in electrical engineering from the University of Alcal (UAH), Madrid, Spain, in 2001. He is currently a Full Professor with the Department of Computer Engineering, University of Alcala (UAH). His research interests include autonomous vehicles and prediction of intentions. He has served as a Project Evaluator, a Rapporteur, and a reviewer for European Commission in the field of ICT for Intelligent Vehicles and Cooperative Systems in FP6 and FP7. He is a member of the IEEE ITSS Board of Governors and Executive Committee. He served as the Editor-in-Chief of *IEEE Intelligent Transportation Systems Magazine*, the Editor-in-Chief of the ITSS Newsletter, and an Associate Editor for IEEE TRANSACTIONS ON INTELLIGENT TRANSPORTATION SYSTEMS. At present, he is the President of the IEEE Intelligent Transportation Systems Society.